Ultrathin Polymer Films: Rubbery Stiffening, Fragility, and Tg

ARTICLE *in* MACROMOLECULES · AUGUST 2015

Impact Factor: 5.8 · DOI: 10.1021/acs.macromol.5b01263

2 AUTHORS:

Xiguang Li

Texas Tech University

6 PUBLICATIONS **37** CITATIONS

SEE PROFILE

Gregory B Mckenna

Texas Tech University

334 PUBLICATIONS **8,058** CITATIONS

SEE PROFILE

Macromolecules

Article

pubs.acs.org/Macromolecules

Ultrathin Polymer Films: Rubbery Stiffening, Fragility, and T_g Reduction

Xiguang Li and Gregory B. McKenna*

Whitacre College of Engineering, Department of Chemical Engineering, Texas Tech University, Lubbock, Texas 79409-4121, United States

ABSTRACT: The mechanical and viscoelastic responses of poly(ethyl methacrylate) (PEMA) ultrathin films over thicknesses ranging from 21 to 112 nm have been studied using a nanobubble inflation method. The stress−strain response of the PEMA thin films shows a rubbery stiffening as the film thickness decreases, and the present results are combined with prior measurements of the rubbery stiffening index S for multiple polymers. We find that S is linearly correlated with the dynamic fragility index m. The results are also consistent with expectation from Ngai et al.'s [*J. Polym. Sci., Part B: Polym. Phys.* **2013**, *51* (3)] recent proposition based on his coupling model but do not seem to correlate with the molecular composite concept proposed by Page et al. [*Nano Lett.* **2014**, *14* (5)] as a means to explain the dependence of the rubbery stiffening on chemical structure of the polymer. In addition, we observe a reduction in glass transition temperature of as much as 15.7 K for PEMA films of 21 nm thickness.

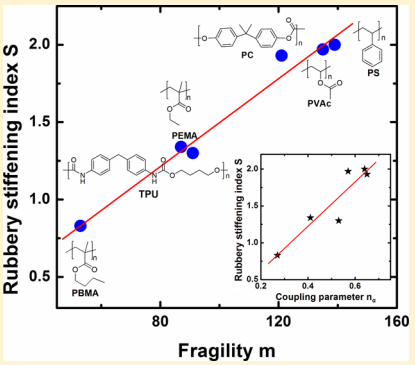

1. INTRODUCTION

The dynamics of small molecules[1] and macromolecules[2−7] confined to nanometer geometries have attracted significant research interest over the past quarter century. Particularly, ultrathin polymer films have been widely studied with the findings of increased,[2,8] unchanged,[9] or reduced T_g [10−13] for thin films supported on substrates. In the case of free-standing polymer thin films, a stronger reduction in the T_g of polystyrene has been observed using ellipsometry and Brillouin scattering.[3] The case of the bubble inflation measurements[14−16] has shown that the reductions for polystyrene, at least, seem to be greater than for the supported films and less than for the ellipsometry measurements. The reasons for this are not currently understood. Of interest in the present work, however, are the reports from our laboratories in which an enhanced stiffness is found for free-standing polymer thin films, both above the thin film reduced T_g and the macroscopic T_g [14,15,17,18] (we name it "rubbery stiffening"). Compared to the macroscopic values, the rubbery stiffness was found to increase by 2−3 orders of magnitude for the thinnest films, scaling with approximately inverse first or second power of the thickness of polymer films, depending on polymer type. It has been suggested that this stiffening phenomenon should be attributed to the surface tension becoming important at the nanoscale. For example, Cuenot and co-workers reported increased room temperature elastic modulus for silver nanowires[19] and polypyrrole nanotubes[20] as diameter decreases, and they attributed these results to be due to the surface tension. However, O'Connell and McKenna[21] showed that the contribution of surface tension does not account for rubbery stiffening of polymer thin films. Furthermore, McKenna and co-workers reported that the surface tensions of poly(vinyl acetate) (PVAc)[21] and poly(*n*-butyl methacrylate) (PBMA) thin films[17] are independent of thickness. And recently, Zhai and McKenna reported similar results for the surface tension of a segmented polyurethane thin film (Estane).[18] Therefore, the rubbery stiffening has been attributed to a nanoconfinement effect,[17,21] although the detailed origins are still unclear. Two models of such stiffening have appeared recently in the literature and will be discussed subsequently.

Examination of the prior work shows that the inherent differences in the chemical structure of the polymers seem to lead to different thickness dependences for the rubbery stiffening. In that work, the slopes S obtained from linear fits of log biaxial compliance vs log thickness were used to describe the thickness dependence, and here we refer to it as the rubbery stiffening index S. It was found that S = 2 for polystyrene (PS)[22] and poly(vinyl acetate) (PVAc),[5] S = 1.93 for polycarbonate (PC),[15] S = 1.3 for segmented polyurethane (Estane),[18] and S = 0.83 for poly(*n*-butyl methacrylate) (PBMA).[17]

Ngai et al. were the first to offer a theoretical framework to explain these results using the coupling model,[23] where they suggested that the strength of rubbery stiffening was related to the extent of the separation of the segmental α relaxation (shape of the stretched exponential fit to the data) and the Rouse modes through the segmental coupling parameter n_α. Recently, Zhai and McKenna,[18] in their work on a segmented polyurethane (Estane) thin film, found that the set of just mentioned polymers seemed to order as expected from the Ngai et al.[23] coupling model.

Received: June 10, 2015
Revised: August 1, 2015
Published: August 18, 2015

DOI: 10.1021/acs.macromol.5b01263
Macromolecules 2015, 48, 6329−6336

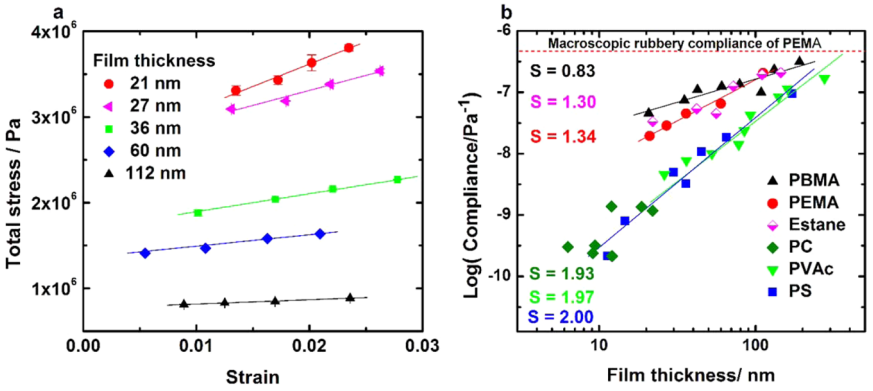

Figure 1. (a) Stress−strain responses for PEMA thin films above the macroscopic glass transition temperature and in the rubbery state. (b) Rubbery biaxial compliance vs film thickness for different polymers.

The work of Ngai et al. has suggested that the origin of the rubbery stiffening can be investigated from the point view of the macroscopic polymer viscoelasticity. In the present work we both examine the proposal of Ngai et al. and go beyond this by considering new data for PEMA thin films. Further we investigate the correlation between rubbery stiffening index S and other glass related parameters, such as dynamic fragility m.[24] Also, we look at a molecular composite concept developed by Page et al. for Nafion films[25] and used to explain the stiffening of polystyrene films. We conclude that the full range of rubbery stiffening results are not consistent with this model. Finally we also show that poly(ethyl methacrylate) (PEMA) ultrathin films exhibit a glass transition temperature (T_g) that decreases as film thickness decreases. The T_g dependence of the PEMA is weaker than that of PS and PC but stronger than that of PVAc.

2. EXPERIMENTS

2.1. Materials and Methods. Poly(ethyl methacrylate) was purchased from Sigma-Aldrich (PEMA, 80% syndiotactic, T_g = 65 °C, M_w = 515K, PDI = 1.52).

PEMA/toluene (ACS reagent grade) solutions (0.5%−2.1%, w/w) were spin-coated onto fresh cut mica sheets at a speed of 2000 rpm for 30 s and then dried for 30 min at room temperature. The films were floated onto a water surface and lifted onto clean silicon nitride filter templates etched with arrays of through channels having diameters of 5 or 10 μm for the present study. The PEMA thin films were dried in a desiccator overnight and annealed at the T_g of each thin film + 15 K for 15 min to bond the films to the template surface. The various film thicknesses were controlled by changing the concentration of PEMA/toluene solution and measured by scoring the template edges and using an atomic force microscope (AFM) (Agilent SPM5500) to measure the step height.[26,27]

The TTU nanobubble inflation method has been described thoroughly in prior works.[26,27] The filter template holding the thin film is mounted in a custom pressure cell using an adhesive and pressurized dry air is applied below the filter template to inflate the sample films into bubbles. The AFM is used to measure the bubble profiles. The AFM (Agilent SPM5500) was operated in intermittent contact mode, and the scan area was 40 × 40 and 20 × 20 μm^2. The scan rate was 1.1 lines/s.

2.2. Data Analysis. To measure the stiffness in the rubbery regime, the PEMA thin films were inflated by stepwise changes in pressure, and the stress−strain response was obtained from the bubble shape and the applied pressure using equations described in previous work.[14,17,27,28] The data is the average for four bubbles. When the bubble deflections are larger than 3 times the film thickness-(membrane limit[29]), the bending contribution is negligible, and the bubble is dominated by the stretching stress.[27] In this case, the bubble shape can be described by a hemisphere. By fitting the bubble profile data to the equation of a circle, the radius of curvature R is calculated as[5,26]

$$R^2 = (x - a)^2 + (y - b)^2 \quad (1)$$

where x and y are the x-position and y-height data, and a and b are offset constants for a circle not centered on the coordinate axes. The stress σ is related to the pressure P, the film thickness t_0, and the radius of curvature R of the bubble as eq 2:[5,26]

$$\sigma_{11} = \sigma_{22} = \frac{PR}{2t_0} \quad (2)$$

The biaxial strain $\varepsilon_{11} = \varepsilon_{22}$ is related to the geometry of the bubble by eqs 3 and 4:[5,26]

$$\varepsilon_{11} = \varepsilon_{22} = \frac{s}{2R_0} - 1 \quad (3)$$

$$s = 2R \sin^{-1}(R_0/R) \quad (4)$$

where R_0 is hole radius and s is the segment length of the bubble.

3. RESULTS AND DISCUSSION

3.1. Rubbery Stiffening Results of PEMA Thin Films. The stress−strain responses for PEMA thin films for thicknesses ranging from 110 to 21 nm are shown in Figure 1a for 85, 85, 85, 80, and 70 °C. These temperatures are above the macroscopic T_g but are not constant because for the thinner films the T_g decreases and the higher temperatures could not be used for the testing due to experimental difficulties. The linear relationship between stress and strain seen in the figure can be described using eq 5:[17,21]

$$\sigma_{total} = \sigma_{11} = E_{biax}\varepsilon_{11} + \sigma_0 \quad (5)$$

where E_{biax} is the biaxial rubbery modulus and σ_0 is the surface stress due to the surface energy of PEMA. As shown in Figure 1a, the rubbery modulus obtained from the slope of the stress−strain data increases as the PEMA film thickness decreases, indicating a rubbery stiffening phenomenon.

To follow the prior works, we determine the rubbery stiffening index S of the polymer thin films by determining the biaxial rubbery compliance as the reciprocal of the biaxial rubbery modulus and plotting it vs the film thickness. A positive slope S is obtained from the fit of log biaxial rubbery compliance vs log thickness. Figure 1b depicts such data for the multiple polymers examined to date. The figure shows that the compliances of the PEMA thin films fall below the macroscopic value and decrease with decreasing film thickness.

DOI: 10.1021/acs.macromol.5b01263
Macromolecules 2015, 48, 6329−6336

The rubbery stiffening index S is 1.34 for the PEMA. The stiffening behavior with decreasing film thickness for the PEMA is compared with that of PS,[14] PVAc,[14] PC,[15] Estane,[18] and PBMA[17] in Figure 1b. The rubbery stiffening index S of PEMA is similar to that of Estane, higher than that of PBMA but lower than those of PS, PVAc, and PC. The values of S are also collected in Table 1. We recognize that there is significant

Table 1. Glass-Forming Properties for Several Polymers with Rubbery Stiffening Index S[a]

polymer	S	m	T_g/K	n_α	S/n_α	m/S
PBMA	0.83	53[34]	305	0.27[38]	3.07	63.8
PEMA	1.34	87[35]	344	0.41[38]	3.27	64.9
Estane	1.3	91[18]	248	0.53[18]	2.45	70
PVAc	1.97	135[36]	311	0.57[23]	3.46	68.5
PC	1.93	121[37]	423	0.65[23]	2.82	66.1
PS	2	139[39,40]	375	0.64[23]	3.12	69.5

[a]The fragility m of PBMA,[34] PEMA,[35] Estane,[18] PVAc,[36] and PC[37] are calculated from the time−temperature shift factors from the viscoelastic data provided in the literature.

work[30,31] showing that the entanglement density decreases as the polymer film thickness decreases, which is not consistent with the observed rubbery stiffening. This is the reason that one needs to search further for the origins of the stiffening. In the case of the present work, we have shown that there are correlations with macroscopic segmental relaxation or the fragility index and these are shown in the next sections.

3.2. Origins of Rubbery Stiffening: Ngai's Coupling Model. For the viscoelasticity of bulk polymers, Plazek and co-workers found a breakdown of thermorheological simplicity,[32,33] and this thermorheological complexity has been attributed to the existence of the α relaxation, the sub-Rouse modes, and the Rouse modes, each having different temperature dependences.[33] Recently, Ngai et al.[23] claimed that the separation of α relaxation and the Rouse modes as well as the separation of the sub-Rouse modes from the Rouse modes in polymer thin films provides an explanation of the rubbery stiffening phenomenon for polymer thin films. They postulated that the segmental α relaxation coupling parameter n_α indicates the extent of this separation, and this is consistent with the rubbery stiffening dependence on thickness observed for PS, PVAc,[14] PC,[15] and PBMA.[17] Zhai and McKenna have reported that the rubbery stiffening of a segmented polyurethane (Estane)[18] follows an ordering that is consistent with Ngai, Prevosto, and Grassia's[23] expectation.

In Figure 2, we see that the rubbery stiffening index S is linearly correlated with n_α of these polymers, which is in a good agreement with Ngai et al.'s expectation.[23] Literature values of coupling parameter n_α, glass transition temperature T_g, and dynamic fragility m are listed in Table 1. In Table 1 we also show the interesting result that the ratio of $S/n_\alpha \approx 3$ for all the polymers so far investigated.

Although the linear correlation of the coupling parameter n_α with the rubbery stiffening index S is reasonable, there are some limitations in the determination on this correlation, e.g., the overlap of α and β relaxations. For some polymers, a large β relaxation may make the n_α value uncertain. Hence, it is of interest to examine other parameters related to glasses. For example, as shown in the inset of Figure 2, the coupling parameter n_α is linearly correlated with dynamic fragility index m, as was reported by Plazek and Ngai.[41] Therefore, it is of

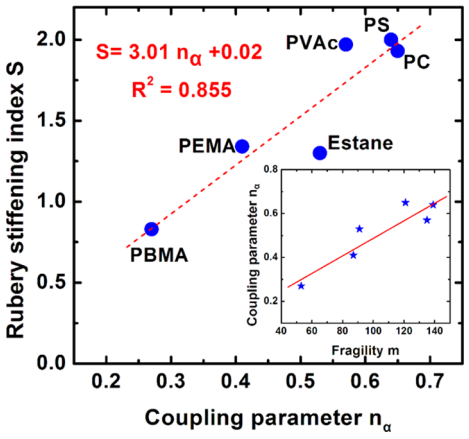

Figure 2. Rubbery stiffening index S vs coupling parameter n_α (inset: the plot of coupling parameter n_α vs fragility m for the same polymers).

interest to examine the relationship between rubbery stiffening index S and dynamic fragility m for these glass-forming polymers.

3.3. Correlation between Rubbery Stiffening and Dynamic Fragility *m*. The dynamic fragility m[24,42] has been used to quantify the rapidity with which a liquid's dynamic properties such as segmental relaxation time or viscosity change as T_g is approached. The relevant equation is[41]

$$m = \left[\frac{\mathrm{d}\log x}{\mathrm{d}\left(\frac{T_g}{T}\right)}\right]_{T=T_g} \tag{6}$$

where x can be segmental relaxation time or viscosity. The dynamic fragility m is related to deviations from an Arrhenius temperature dependence of the relaxation properties, and the Vogel−Fulcher−Tammann (VFT) relation for the glass forming liquids (eq 7)[43−45] can be used to obtain the dynamic fragility m as shown in eq 8.[46]

$$\tau = \tau_\infty \exp\left(\frac{B}{T - T_\infty}\right) \tag{7}$$

$$m = \frac{BT_g}{\ln 10(T_g - T_\infty)^2} \tag{8}$$

where τ_∞ and B are material-dependent constants and T_∞ is the temperature at which the viscosity or relaxation time become infinite. Although useful, the value of dynamic fragility can depend on the measurement method. For example, the fragility value of PVAc determined by dielectric measurement ($m = 91$) is smaller than that obtained from mechanical testing ($m = 135$). McKenna and co-workers[47−49] reported that, in fact, the dielectric response of PVAc follows the same temperature dependence as the terminal dispersion of the mechanical response, rather than the segmental dispersion. Interestingly, Ngai et al.[50] have reported that for PVAc both the B parameter in the VFT equation and the exponent β of the stretched exponential equation depend on the measurement method. The observations were reconciled within the context of the coupling model. Hence, for consistency in the present work, we use fragility values determined from viscoelastic measurements in the region of the segmental relaxation, rather than dielectric or DSC measurements.

DOI: 10.1021/acs.macromol.5b01263
Macromolecules 2015, 48, 6329−6336

Very interestingly, the correlation between dynamic fragility m and rubbery stiffening index S is found to be strong. Table 1 shows that fragility m is related to the rubbery stiffening index S with a ratio of 65−70, and Figure 3 also demonstrates the linear

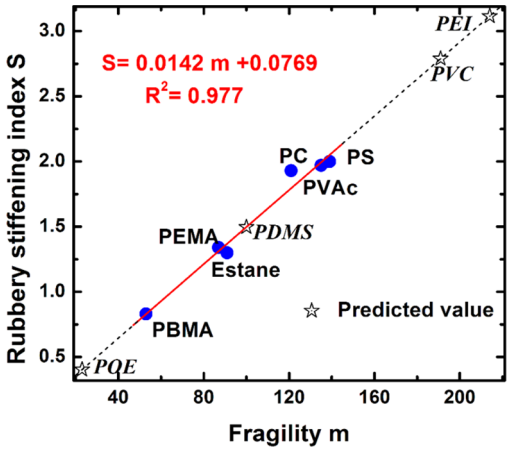

Figure 3. Plot of rubbery stiffening index vs dynamic fragility showing the linear correlation between the two: (solid circles) experimental data; (stars) estimated values from correlation line and fragility m.

correlation between rubbery stiffening index S and dynamic fragility m. Fragile polymers such as polystyrene and polycarbonate show a high rubbery stiffening index S, and "strong" polymers such as PBMA exhibit a low rubbery stiffening index. Sokolov and co-workers suggested that the stiffness of the side group relative to backbone is the major factor to control the fragility of polymers.[51] Here we propose that the rubbery stiffening index S of polymers might have a similar origin; however, more quantitative work on the stiffness and conformational activation energy of the side chains and backbones of polymers is required to further elucidate this speculation.

One advantage of our correlation approach is that we can use the abundant literature data of dynamic fragility m to "predict" the rubbery stiffening index of free-standing polymer thin films that have not yet been tested. Shown in Figure 3, one could predict that the medium fragile PDMS (m = 100[52]) and highly fragile PVC (m = 191[53]) would have rubbery stiffening indexes S of 1.50 and 2.79, respectively. Furthermore, the fragility values for poly(ether imide) (m = 214[46]) and poly(oxyethylene) (m = 23[53]) would predict upper (S = 3.12) and lower bounds (S = 0.40) for the rubbery stiffening behavior of polymers.

3.4. Origins of Rubbery Stiffening: Molecular Composite Concept Based on Molecular Properties of Polymers. Another possible explanation for the rubbery stiffening is based on the contributions of the stiffness of the polymer chains themselves. Page et al.[25] have provided a molecular composite concept incorporating the stiffness of a single polymer chain. Since the single polymer chain is much stiffer than the bulk polymer,[54] Page et al. consider the single polymer chain as a reinforcing element[25] and treat the thin films as a composite of soft bulk polymer and rigid single chain using a modified Halpin−Tsai equation.[55] As Page et al.[25] proposed, the fraction of the single chain (rigid phase) increases with decreasing film thickness; hence, the film stiffness increases.

Here we use literature data for polymer chain stiffness and our rubbery stiffening results to examine the above molecular composite concept. Back to the 1970s, X-ray diffraction[56,57] and Raman spectroscopy[58,59] were used to determine the stiffness of local crystalline regions, thought to give a good estimation of the stiffness of aligned polymer chains. Tashiro[60] summarized the factors governing the polymer chain stiffness, and we present the literature values of some polymers along with the monomer chemical structure in Table 2. Two points are worth remarking upon. First, the backbone conformation is the most dominant factor for chain stiffness. The planar zigzag conformation usually gives a much higher stiffness compared to that of the helical conformation;[60] e.g., PE (planar zigzag) has a higher stiffness of 240 GPa than does PP (3/1 helix, 40 GPa). Second, intermolecular interactions through side groups have weak effects on the chain stiffness compared to the backbone.[60] With similar chemical structure, PEMA was reported to have a similar local helix structure to PMMA;[61] therefore, it is reasonable to assume that PEMA has a similar chain stiffness to PMMA (10 GPa). And we also assume PC has a similar chain stiffness to PET (118 GPa) due to their similar aromatic backbones. At the same time, bulky side groups can decrease the chain stiffness because of the large cross-sectional area, e.g. PS.[56]

In Figure 4, the tensile modulus of PS, PEMA, and PC is plotted as a function of film thickness, marked with their chain stiffness E_c. As Page et al.[25] proposed in their molecular composite model, the upper bound values for the rubbery stiffening are the individual chain stiffnesses of the polymers. However, our rubbery stiffening results and chain stiffness data are not consistent with the molecular composite model. PC has a much higher chain stiffness E_c than PS, but its data fall into the range of the predicted curves for PS. PS and PEMA have similar chain stiffness E_c (similar upper bounds), but the PEMA data are below the model predictions for PS. Therefore, our

Table 2. Chain Stiffness of Some Polymers

Polymer	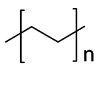 PE	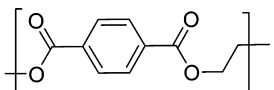 PET	 PS	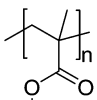 PEMA	 PMMA
Chain stiffness E_c	240 GPa Planar, zig-zag[56, 60]	118 GPa Planar zig-zag[60]	12 GPa Isotactic, helix[56]	Similar to PMMA[61]	10 GPa Isotactic, helix[62]

DOI: 10.1021/acs.macromol.5b01263
Macromolecules 2015, 48, 6329−6336

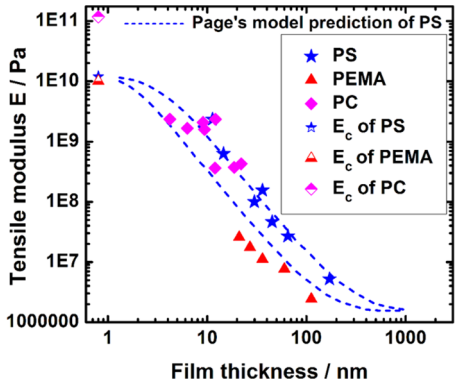

Figure 4. Rubbery stiffening of PS, PEMA, and PC thin films as a function of thickness compared with their chain stiffness E_c. Dashed lines are reproduced from Page et al.[25]

results are not consistent with the molecular composite model. The reason might be that the interchain interaction is important for rubbery stiffening behavior. On the other hand, for both fragility and the Ngai et al. model, the interchain cooperativity related to the interchain interaction is an important factor related to glass-formation properties, something which is neglected in the single chain stiffness-based composite model.

3.5. Creep Behavior and T_g Reduction. The nanobubble inflation method can also be used to determine the T_g of the PEMA thin films. Figure 5a shows a series of center-line profiles for a 21 nm thick PEMA film at 50 °C at an inflation pressure of 20.3 kPa, obtained at different times. From the profiles we see that the capillary forces have drawn the film into the holes, and the boundaries of the bubbles are below the substrate surface. This occurs during the film annealing process and has been discussed previously.[26,27] As shown in Figure 5a, the 21 nm thick PEMA bubble continues to grow with time at 50 °C, illustrating a creep behavior below the macroscopic T_g of 65 °C. To represent the creep results for a range of temperatures, we choose the reference curves in the glass transition region and then shift the other apparent creep compliance curves to construct a master curve using time−temperature superposition.[63] Figure 5b shows PEMA creep master curves for film thickness ranging from 21 to 112 nm. Two trends can be observed. First, when the film thickness is below 30 nm, PEMA can creep below the macroscopic T_g of 65 °C, hence indicating a T_g depression. Second is that the rubbery plateau stiffens significantly as the film thickness decreases. Since the reference temperature for each master curve is somewhat arbitrarily chosen, we show a quantitative determination of T_g in the next paragraph.

The glass transition temperatures were determined using the following procedure: For each thickness, the creep results at different temperatures were fitted to obtain retardation times using the modified Kohlrausch−Williams−Watts (KWW) equation[64]

$$D(t) = D_g + D_N\left[1 - \exp\left(-\left(\frac{t}{\tau}\right)^{\beta}\right)\right] \quad (9)$$

where D_g is the glassy biaxial compliance (2×10^{-10} Pa^{-1} from macroscopic data) and D_N is the rubbery plateau biaxial compliance. τ and β are the retardation time and the stretching exponent, respectively, which can be obtained as fitting parameters. For a 112 nm thick PEMA film, the retardation time τ was obtained as 1×10^5 s at 65 °C, and we assume the 112 nm thick film has the same T_g as the macroscopic T_g of 65 °C. Therefore, 1×10^5 s is chosen as the reference retardation time τ_{ref}, and all shift factors are obtained using $a_T = \tau/\tau_{ref}$. To determine the reduction of T_g of PEMA quantitatively, the temperature shift factors a_T vs the reciprocal temperature are plotted for each thickness and fitted using the Vogel−Fulcher−Tammann equation (VFT)[43−45] in Figure 6a. For each thickness, the T_g was determined as the temperature with the shift factor a_T equaling to zero, using the VFT equation. Table 3 lists the VFT parameters for the PEMA thin films. From the curves in Figure 6a it is clear that the PEMA thin films show a weaker temperature dependence and different VFT parameters (see also Table 3) compared to the bulk PEMA. This is different from the nanobubble inflation results of free-standing PS, PVAc,[14] and PC thin films,[15] which seemed to exhibit reductions in the T_g but only a shifted temperature dependence of the curves, i.e., a reduction in T_∞ and no change in the curve shapes. Importantly, the results at that time were more scattered than those determined here. Also of interest is that supported thin films have been reported to exhibit different

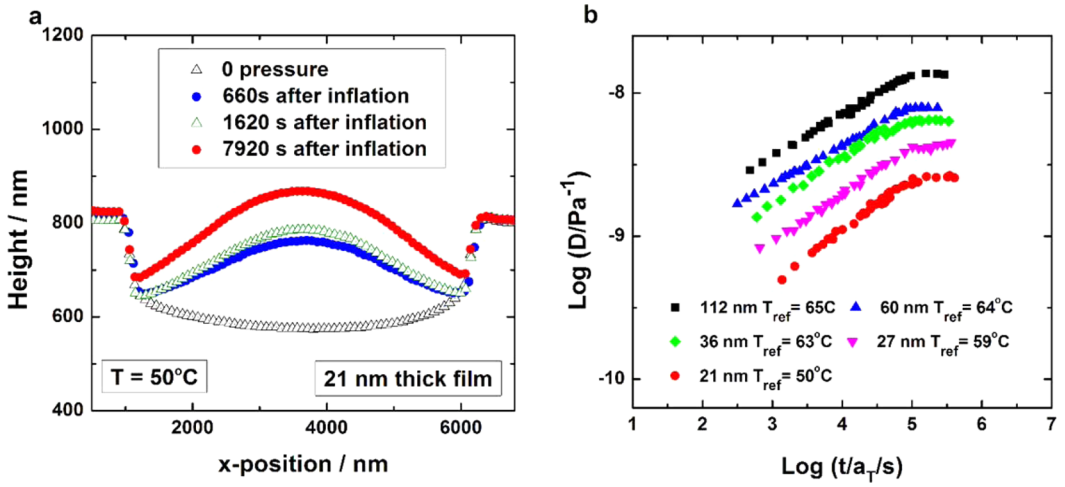

Figure 5. (a) Creep profiles of 5 μm diameter bubbles for a 21 nm thick PEMA film at 50 °C with the pressure of 20.3 kPa at different creep times. (b) Creep master curves for PEMA thin films of differing thickness.

DOI: 10.1021/acs.macromol.5b01263
Macromolecules 2015, 48, 6329−6336

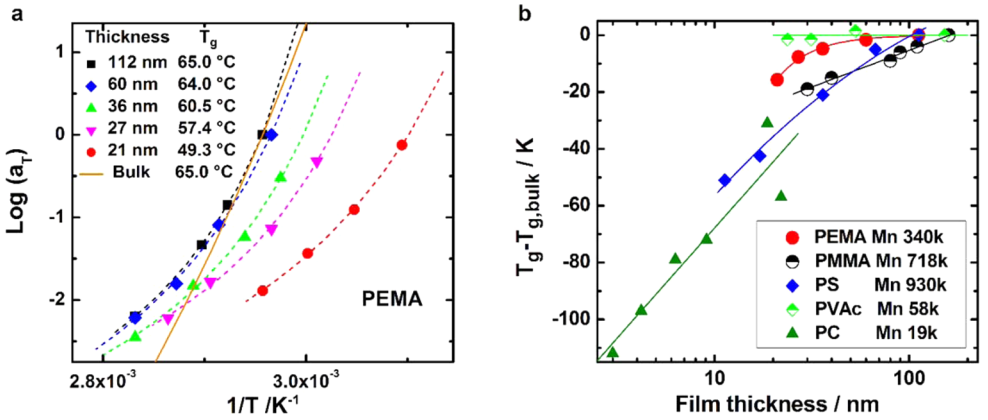

Figure 6. (a) Time−temperature shift factors vs $1/T$ for PEMA thin films. Dashed lines are the VFT fitting curves and solid line is macroscopic PEMA VFT curve.[35] (b) T_g reduction as a function of film thickness for the PEMA compared with results for PMMA,[3] PS, PVAc,[14] and PC.[15]

Table 3. VFT Parameters and Glass-Forming Properties for PEMA Thin Films

thickness/nm	B	T_∞/K	T_g/K	m
macroscopic PEMA[35]	2983	267.0	338.2	87
112	237	318.1	338.2	86.8
60	298	313.7	337.2	79.7
36	250	312.3	333.6	78.9
27	241	308.6	330.6	71.8
21	310	295.9	322.4	61.6

VFT behaviors from the macroscopic, but with strongly decreased values of T_∞ as film thickness decreases.[10,65,66] This is not the case here. In addition, the surface dynamics have been reported to show different VFT behavior from that of the macroscopic dynamics. For example, particle embedment studies, e.g. Yoon and McKenna,[11] show a much stronger behavior in the fragility sense for the surface viscoelasticity than the bulk behavior, and previous hole refilling experiments of Fakhraai and Forrest[67] show similar "strengthening" of the temperature dependence of the surface dynamic response. There is also other nanoscale confinement leading to stronger Arrhenius-like dynamics, e.g. glass-forming liquids in nanopores.[68] For the present work it is of interest that the change of the VFT B and T_∞ values compensate to give the same m at unchanged T_g for the 112 nm thick film compared to the bulk value.

The reduction of T_g as a function of film thickness is shown in Figure 6b. For comparison, the ΔT_g vs free-standing film thickness for PS,[14] PVAc,[14] and PC[15] reported by McKenna and co-workers using nanobubble inflation is also plotted. As seen, the PEMA has a weaker T_g reduction than PS or PC but greater than that of PVAc. The results of free-standing atactic PMMA reported by Roth and Dutcher using ellipsometry[3] are also shown for comparison. Although both PEMA and PMMA belong to the family of poly(alkyl methacrylates), and their extents of T_g reduction are similar when the thickness decreases from 120 to 20 nm, the trend is different since PEMA only shows a significant T_g reduction when the thickness approaches 30 nm. This supports the thought that the thickness dependence of T_g reductions in freely standing polymer thin films depends on the chemical structure of the polymer, as O'Connell and McKenna reported.[14] Here it is important to keep in mind that the ellipsometry results do not show the exact same temperature dependence of the T_g reduction with film thickness for polystyrene as seen in multiple compilations of T_g reduction data.[10,13] It is also important to recognize new data from the Roth group[69] using ellipsometry that not only shows that there are differences between the mechanical estimates of T_g reduction and the ellipsometric measurements but also suggests the possibility that the ellipsometry is seeing two different glass transitions in the freely standing films. This latter has been seen in nanoporous confinement[70,71] but not in supported films and that puts some question into the differences in the pseudothermodynamic measurements[4] such as ellipsometry and the direct dynamic measurements such as dielectric spectroscopy[65] or the viscoelastic measurements used here.

4. CONCLUSIONS

The mechanical and viscoelastic responses of poly(ethyl methacrylate) (PEMA) ultrathin films over thicknesses ranging from 21 to 112 nm have been studied using a nanobubble inflation method. The present results are combined with prior measurements of the rubbery stiffening index S for multiple polymers, and they are found to be linearly correlated with the segmental α relaxation coupling parameter n_α from Ngai's coupling model and with the dynamic fragility index m. We also compare Page et al.'s molecular composite concept that incorporates the stiffness of a single polymer chain and find that our experimental results are not consistent with their molecular composite concept. Overall, the results presented are consistent with the idea that the temperature dependence related to glass formation, or the structural relaxation itself, plays an important role in the thin film "rubbery" stiffening. We also find that the glass transition temperature (T_g) of PEMA decreases by as much as 15.7 K for a 21 nm thick, freely standing film—a trend weaker than found in PS or PC but stronger than PVAc. PEMA free-standing thin films have a somewhat different T_g reduction behavior compared to the results of free-standing PMMA thin films using ellipsometry[3] and also exhibit a weaker temperature dependence and different VFT parameters compared to the macroscopic PEMA, but with only a weak change in fragility index.

AUTHOR INFORMATION

Corresponding Author

*E-mail greg.mckenna@ttu.edu (G.B.M.).

Notes

The authors declare no competing financial interest.

DOI: 10.1021/acs.macromol.5b01263
Macromolecules 2015, 48, 6329−6336

■ ACKNOWLEDGMENTS

The authors are grateful to the National Science Foundation under Grant DMR-1207070 and to the John R. Bradford Endowment at Texas Tech University, each for partial financial support of this work.

■ REFERENCES

(1) Jackson, C. L.; McKenna, G. B. The glass transition of organic liquids confined to small pores. *J. Non-Cryst. Solids* **1991**, *131−133* (Part 1), 221−224.
(2) Keddie, J. L.; Jones, R. A. L.; Cory, R. A. Interface and surface effects on the glass-transition temperature in thin polymer films. *Faraday Discuss.* **1994**, *98*, 219−230.
(3) Roth, C. B.; Dutcher, J. R. Glass transition temperature of freely-standing films of atactic poly(methyl methacrylate). *Eur. Phys. J. E: Soft Matter Biol. Phys.* **2003**, *12* (Suppl 1), 103−7.
(4) Alcoutlabi, M.; McKenna, G. B. Effects of confinement on material behaviour at the nanometre size scale. *J. Phys.: Condens. Matter* **2005**, *17* (15), R461−R524.
(5) O'Connell, P. A.; McKenna, G. B. Rheological measurements of the thermoviscoetastic response of ultrathin polymer films. *Science* **2005**, *307*, 1760−1763.
(6) Ediger, M. D.; Forrest, J. A. Dynamics near Free Surfaces and the Glass Transition in Thin Polymer Films: A View to the Future. *Macromolecules* **2014**, *47* (2), 471−478.
(7) Chai, Y.; Salez, T.; McGraw, J. D.; Benzaquen, M.; Dalnoki-Veress, K.; Raphaël, E.; Forrest, J. A. A Direct Quantitative Measure of Surface Mobility in a Glassy Polymer. *Science* **2014**, *343* (6174), 994−999.
(8) Grohens, Y.; Hamon, L.; Reiter, G.; Soldera, A.; Holl, Y. Some relevant parameters affecting the glass transition of supported ultra-thin polymer films. *Eur. Phys. J. E: Soft Matter Biol. Phys.* **2002**, *8* (2), 217−24.
(9) Tress, M.; Erber, M.; Mapesa, E. U.; Huth, H.; Müller, J.; Serghei, A.; Schick, C.; Eichhorn, K.-J.; Voit, B.; Kremer, F. Glassy Dynamics and Glass Transition in Nanometric Thin Layers of Polystyrene. *Macromolecules* **2010**, *43* (23), 9937−9944.
(10) Gao, S.; Koh, Y. P.; Simon, S. L. Calorimetric Glass Transition of Single Polystyrene Ultrathin Films. *Macromolecules* **2013**, *46* (2), 562−570.
(11) Yoon, H.; McKenna, G. B. Substrate Effects on Glass Transition and Free Surface Viscoelasticity of Ultrathin Polystyrene Films. *Macromolecules* **2014**, *47* (24), 8808−8818.
(12) Evans, C. M.; Deng, H.; Jager, W. F.; Torkelson, J. M. Fragility is a Key Parameter in Determining the Magnitude of Tg-Confinement Effects in Polymer Films. *Macromolecules* **2013**, *46* (15), 6091−6103.
(13) Wang, J.; McKenna, G. B. Viscoelastic and Glass Transition Properties of Ultrathin Polystyrene Films by Dewetting from Liquid Glycerol. *Macromolecules* **2013**, *46* (6), 2485−2495.
(14) O'Connell, P. A.; Hutcheson, S. A.; McKenna, G. B. Creep behavior of ultra-thin polymer films. *J. Polym. Sci., Part B: Polym. Phys.* **2008**, *46* (18), 1952−1965.
(15) O'Connell, P. A.; Wang, J.; Ishola, T. A.; McKenna, G. B. Exceptional Property Changes in Ultrathin Films of Polycarbonate: Glass Temperature, Rubbery Stiffening, and Flow. *Macromolecules* **2012**, *45* (5), 2453−2459.
(16) Xu, S.; O'Connell, P. A.; McKenna, G. B.; Castagnet, S. Nanomechanical properties in ultrathin polymer films: Measurement on rectangular versus circular bubbles. *J. Polym. Sci., Part B: Polym. Phys.* **2012**, *50* (7), 466−476.
(17) Xu, S.; O'Connell, P. A.; McKenna, G. B. Unusual elastic behavior of ultrathin polymer films: Confinement-induced/molecular stiffening and surface tension effects. *J. Chem. Phys.* **2010**, *132* (18), 184902.
(18) Zhai, M.; McKenna, G. B. Elastic modulus and surface tension of a polyurethane rubber in nanometer thick films. *Polymer* **2014**, *55*, 2725−2733.
(19) Cuenot, S.; Frétigny, C.; Demoustier-Champagne, S.; Nysten, B. Surface tension effect on the mechanical properties of nanomaterials measured by atomic force microscopy. *Phys. Rev. B: Condens. Matter Mater. Phys.* **2004**, *69* (16), 165410.
(20) Cuenot, S.; Demoustier-Champagne, S.; Nysten, B. Elastic Modulus of Polypyrrole Nanotubes. *Phys. Rev. Lett.* **2000**, *85* (8), 1690−1693.
(21) O'Connell, P. A.; McKenna, G. B. The stiffening of ultrathin polymer films in the rubbery regime: The relative contributions of membrane stress and surface tension. *J. Polym. Sci., Part B: Polym. Phys.* **2009**, *47* (24), 2441−2448.
(22) O'Connell, P. A.; McKenna, G. B. Dramatic stiffening of ultrathin polymer films in the rubbery regime. *Eur. Phys. J. E: Soft Matter Biol. Phys.* **2006**, *20* (2), 143−150.
(23) Ngai, K. L.; Prevosto, D.; Grassia, L. Viscoelasticity of nanobubble-inflated ultrathin polymer films: Justification by the coupling model. *J. Polym. Sci., Part B: Polym. Phys.* **2013**, *51* (3), 214−224.
(24) Angell, C. A. Relaxation in liquids, polymers and plastic crystals — strong/fragile patterns and problems. *J. Non-Cryst. Solids* **1991**, *131−133* (Part 1), 13−31.
(25) Page, K. A.; Kusoglu, A.; Stafford, C. M.; Kim, S.; Kline, R. J.; Weber, A. Z. Confinement-driven increase in ionomer thin-film modulus. *Nano Lett.* **2014**, *14* (5), 2299−304.
(26) O'Connell, P. A.; McKenna, G. B. Novel nanobubble inflation method for determining the viscoelastic properties of ultrathin polymer films. *Rev. Sci. Instrum.* **2007**, *78* (1), 013901.
(27) O'Connell, P. A.; McKenna, G. B. A novel nano-bubble inflation method for determining the viscoelastic properties of ultrathin polymer films. *Scanning* **2008**, *30* (2), 184−196.
(28) Li, X.; Warzywoda, J.; McKenna, G. B. Mechanical responses of a polymer graphene-sheet nano-sandwich. *Polymer* **2014**, *55* (19), 4976−4982.
(29) Timoshenko, S. P.; Woinowsky-Krieger, S. *Theory of Plates and Shells*; McGraw-Hill: New York, 1969.
(30) Brown, H. R.; Russell, T. P. Entanglements at Polymer Surfaces and Interfaces. *Macromolecules* **1996**, *29* (2), 798−800.
(31) Si, L.; Massa, M. V.; Dalnoki-Veress, K.; Brown, H. R.; Jones, R. A. L. Chain Entanglement in Thin Freestanding Polymer Films. *Phys. Rev. Lett.* **2005**, *94* (12), 127801.
(32) Plazek, D. J. 1995 Bingham Medal Address: Oh, thermorheological simplicity, wherefore art thou? *J. Rheol.* **1996**, *40* (6), 987.
(33) Plazek, D. J.; Chay, I. C.; Ngai, K. L.; Roland, C. M. Viscoelastic properties of polymers. 4. Thermorheological complexity of the softening dispersion in polyisobutylene. *Macromolecules* **1995**, *28* (19), 6432−6436.
(34) Child, W. C., Jr.; Ferry, J. D. Dynamic mechanical properties of poly-n-butyl methacrylate. *J. Colloid Sci.* **1957**, *12* (3), 327−341.
(35) Ferry, J. D.; Child, W. C., Jr.; Zand, R.; Stern, D. M.; Williams, M. L.; Landel, R. F. Dynamic mechanical properties of polyethyl methacrylate. *J. Colloid Sci.* **1957**, *12* (1), 53−67.
(36) Plazek, D. J. The Temperature Dependence of the Viscoelastic Behavior of Poly(vinyl acetate). *Polym. J.* **1980**, *12* (1), 43−53.
(37) Mercier, J. P.; Aklonis, J. J.; Litt, M.; Tobolsky, A. V. Viscoelastic behavior of the polycarbonate of bisphenol A. *J. Appl. Polym. Sci.* **1965**, *9* (2), 447−459.
(38) Ngai, K. L.; Gopalakrishnan, T. R.; Beiner, M. Relaxation in poly(alkyl methacrylate)s: Change of intermolecular coupling with molecular structure, tacticity, molecular weight, copolymerization, crosslinking, and nanoconfinement. *Polymer* **2006**, *47* (20), 7222−7230.
(39) Ngai, K. L.; Plazek, D. J. A quantitative explanation of the difference in the temperature dependences of the viscoelastic softening and terminal dispersions of linear amorphous polymers. *J. Polym. Sci., Part B: Polym. Phys.* **1986**, *24* (3), 619−632.
(40) Böhmer, R.; Ngai, K. L.; Angell, C. A.; Plazek, D. J. Nonexponential relaxations in strong and fragile glass formers. *J. Chem. Phys.* **1993**, *99* (5), 4201−4209.

DOI: 10.1021/acs.macromol.5b01263
Macromolecules 2015, 48, 6329−6336

(41) Plazek, D. J.; Ngai, K. L. Correlation of polymer segmental chain dynamics with temperature-dependent time-scale shifts. *Macromolecules* **1991**, *24* (5), 1222−1224.
(42) Böhmer, R.; Angell, C. A. Correlations of the nonexponentiality and state dependence of mechanical relaxations with bond connectivity in Ge-As-Se supercooled liquids. *Phys. Rev. B: Condens. Matter Mater. Phys.* **1992**, *45* (17), 10091−10094.
(43) Vogel, H. The law of relation between the viscosity of liquids and the temperature. *Phys. Z.* **1921**, *22*, 645−646.
(44) Fulcher, G. S. Analysis of recent measurements of the viscosity of glasses. *J. Am. Ceram. Soc.* **1925**, *8* (6), 339−355.
(45) Tammann, G.; Hesse, W. The dependence of viscosity upon the temperature of supercooled liquids. *Z. Anorg. Allg. Chem.* **1926**, *156*, 245−257.
(46) Qin, Q.; McKenna, G. B. Correlation between dynamic fragility and glass transition temperature for different classes of glass forming liquids. *J. Non-Cryst. Solids* **2006**, *352* (28−29), 2977−2985.
(47) Kollengodu-Subramanian, S.; McKenna, G. B. A dielectric study of poly(vinyl acetate) using a pulse-probe technique. *J. Therm. Anal. Calorim.* **2010**, *102* (2), 477−484.
(48) Zhao, J.; McKenna, G. B. Temperature divergence of the dynamics of a poly(vinyl acetate) glass: Dielectric vs. mechanical behaviors. *J. Chem. Phys.* **2012**, *136* (15), 154901.
(49) McKenna, G. B.; Zhao, J. Accumulating evidence for non-diverging time-scales in glass-forming fluids. *J. Non-Cryst. Solids* **2015**, *407*, 3−13.
(50) Ngai, K. L.; Mashimo, S.; Fytas, G. Intercomparisons of dielectric relaxation, dynamic light scattering, and viscoelastic properties of the local segmental motion in amorphous polymers. *Macromolecules* **1988**, *21* (10), 3030−3038.
(51) Kunal, K.; Robertson, C. G.; Pawlus, S.; Hahn, S. F.; Sokolov, A. P. Role of Chemical Structure in Fragility of Polymers: A Qualitative Picture. *Macromolecules* **2008**, *41* (19), 7232−7238.
(52) Roland, C. M.; Santangelo, P. G.; Ngai, K. L. The application of the energy landscape model to polymers. *J. Chem. Phys.* **1999**, *111* (12), 5593.
(53) Huang, D.; McKenna, G. B. New insights into the fragility dilemma in liquids. *J. Chem. Phys.* **2001**, *114* (13), 5621−5630.
(54) Holliday, L.; White, J. W. The stiffness of polymers in relation to their structure. *Pure Appl. Chem.* **1971**, *26* (3−4), 545−582.
(55) Halpin, J. C.; Kardos, J. L. The Halpin-Tsai equations: A review. *Polym. Eng. Sci.* **1976**, *16* (5), 344−352.
(56) Sakurada, I.; Ito, T.; Nakamae, K. Elastic moduli of the crystal lattices of polymers. *J. Polym. Sci., Part C: Polym. Symp.* **1967**, *15* (1), 75−91.
(57) Sakurada, I.; Kaji, K. Relation between the polymer conformation and the elastic modulus of the crystalline region of polymer. *J. Polym. Sci., Part C: Polym. Symp.* **1970**, *31* (1), 57−76.
(58) Strobl, G. R.; Eckel, R. A raman spectroscopic determination of the interlamellar forces in crystalline n-alkanes and of the limiting elastic modulus Ec of polyethylene. *J. Polym. Sci., Polym. Phys. Ed.* **1976**, *14* (5), 913−920.
(59) Pietralla, M.; Hotz, R.; Engst, T.; Siems, R. Chain direction elastic modulus of PE crystal and interlamellar force constant of n-alkane crystals from Raman measurements. *J. Polym. Sci., Part B: Polym. Phys.* **1997**, *35* (1), 47−57.
(60) Tashiro, K. Molecular theory of mechanical properties of crystalline polymers. *Prog. Polym. Sci.* **1993**, *18* (3), 377−435.
(61) Wind, M.; Graf, R.; Renker, S.; Spiess, H. W.; Steffen, W. Structure of amorphous poly-(ethylmethacrylate): A wide-angle x-ray scattering study. *J. Chem. Phys.* **2005**, *122* (1), 14906−14915.
(62) Urbanek, S.; Tashiro, K.; Kitayama, T.; Hatada, K. Crystallite modulus of double-stranded helices of isotactic poly(methyl methacrylate): the X-ray measurement and the theoretical calculation. *Polymer* **1999**, *40* (12), 3345−3351.
(63) Ferry, J. D. *Viscoelastic Properties of Polymers*; Wiley: New York, 1980.
(64) Williams, G.; Watts, D. C. Non-symmetrical dielectric relaxation behaviour arising from a simple empirical decay function. *Trans. Faraday Soc.* **1970**, *66* (0), 80−85.
(65) Fukao, K.; Miyamoto, Y. Slow dynamics near glass transitions in thin polymer films. *Phys. Rev. E: Stat. Phys., Plasmas, Fluids, Relat. Interdiscip. Top.* **2001**, *64* (1), 011803.
(66) Yang, Z.; Peng, D.; Clough, A.; Lam, C. H.; Tsui, O. K. C. Is the dynamics of polystyrene films consistent with their glass transition temperature? *Eur. Phys. J.: Spec. Top.* **2010**, *189* (1), 155−164.
(67) Fakhraai, Z.; Forrest, J. A. Measuring the Surface Dynamics of Glassy Polymers. *Science* **2008**, *319* (5863), 600−604.
(68) Mel'nichenko, Y. B.; Schüller, J.; Richert, R.; Ewen, B.; Loong, C. K. Dynamics of hydrogen-bonded liquids confined to mesopores: A dielectric and neutron spectroscopy study. *J. Chem. Phys.* **1995**, *103* (6), 2016−2024.
(69) Pye, J. E.; Roth, C. B. Two Simultaneous Mechanisms Causing Glass Transition Temperature Reductions in High Molecular Weight Freestanding Polymer Films as Measured by Transmission Ellipsometry. *Phys. Rev. Lett.* **2011**, *107* (23), 235701.
(70) Park, J.-Y.; McKenna, G. B. Size and confinement effects on the glass transition behavior of polystyrene/*o*-terphenyl polymer solutions. *Phys. Rev. B: Condens. Matter Mater. Phys.* **2000**, *61* (10), 6667−6676.
(71) Li, L.; Zhou, D.; Huang, D.; Xue, G. Double Glass Transition Temperatures of Poly(methyl methacrylate) Confined in Alumina Nanotube Templates. *Macromolecules* **2014**, *47* (1), 297−303.

DOI: 10.1021/acs.macromol.5b01263
Macromolecules 2015, 48, 6329−6336